



## Duxite – Fossil resin of Miocene age

Martina Havelcová<sup>a,\*</sup>, Vladimír Machovič<sup>a,b</sup>, Ivana Sýkorová<sup>a</sup>, Ladislav Lapčák<sup>b</sup>,  
Alexandra Špaldoňová<sup>a</sup>, Karel Mach<sup>c</sup>, Zdeněk Dvořák<sup>c</sup>

<sup>a</sup> Institute of Rock Structure and Mechanics AS CR, V Holešovičkách 41, 182 09 Praha 8, Czech Republic

<sup>b</sup> University of Chemistry and Technology, Prague, Technická 5, 166 28 Praha 6, Czech Republic

<sup>c</sup> Severočeské doly, a.s., Doly Bílina (North Bohemian Mines, Bílina Mines), 5. května 213, 418 29 Bílina, Czech Republic

### ARTICLE INFO

#### Article history:

Received 27 February 2018

Received in revised form 18 July 2018

Accepted 26 July 2018

Available online 4 August 2018

#### Keywords:

Fossil resin

Amber

Resinite

Terpenoids

Py-GC/MS

FTIR

### ABSTRACT

A series of Miocene fossil resin from the northwest part of the Czech Republic, called duxite, has been analyzed by elemental, microscopic, gas chromatography (GC/MS), pyrolysis-gas chromatography, Fourier Transform infrared (FTIR), and Raman techniques. The set of samples consisted of museum, contemporary and artificially altered samples. The results of GC/MS revealed fine variances in chemical structure among the samples, which could be attributed to the geologic paleosituation during resin deposition, as was verified by alteration of a sample under different conditions. Sesquiterpenes, including  $\alpha$ -cedrene and cuparene, were identified in sample extracts and sample pyrolysates together with diterpenoid members abietanes, pimaranes, and dehydroabietanes. The distribution and intensity of functional groups of FTIR spectra also confirmed that the duxite samples were fossilised exudates from a member of the Cupressaceae conifer family. Raman spectra supported this record indicating aromatic character of duxite and higher maturity of the samples. The chemical composition indicated that duxite is a member of Class IV resins of the fossil resin classification system. Members of this group do not have a polymeric structure. This nonpolymerizable behaviour was confirmed by their excellent solubility in an organic solvent and the low softening point of the material. Our results therefore provide a valuable insight into the duxite-producing process and its potential for evaluating the geological environment and diagenetic conditions.

© 2018 Elsevier Ltd. All rights reserved.

## 1. Introduction

In 1874, the first details of the discovery of a fossilized resin from a Miocene coal seam in the former Emeran Mine of Duchcov in the North Bohemian Basin were published. The substance was named duxite after the German name of the town Dux (Doelter, 1874). The fossilised resin, 2–8 cm thick, was directly connected to coal on each side. The resin was described as an indigenous deposit, dark brown, wax-shiny, brittle with a conchoidal fracture.

Bittner (1913) first described duxite in a mine and later Jurasky (1940) described duxite in the Elly Mine which closed in 1941, in the same region of the North Bohemian Basin, forming fillings of vertical fractures in layers of xylitic coal. Jurasky also published the first concepts about the genesis of duxite, followed by Kuhlwein (1951), both describing the transformation of the resin under the influence of volcanic heat. The resin becomes mobilized by superheated steam at approximately 350 °C (or at a lower

temperature under a high pressure), migrates, and impregnates the surrounding coal material. The geological systems of the Doupovské Mountains and České Středohoří Mountains are connected with an intrusive body that can provide volcanic underground heating over a large area. According to Kuhlwein (1951), other localities where duxite had been found include, the Pluto Mine at Osek and Mariánské Radčice (North Bohemian Basin), the Josef and Anežka Mine (Sokolov Basin), and in a Slovakian bed at Handlová.

Stach (1966), during his coalification studies, also researched duxite. Based on its solubility, melting point, and degree of polymerization, he referred to duxite as black amber. The black colour of the resin was attributed to the presence of humic substances in the coal, and he also assumed that duxite was a product of volcanic and thermal processes. However, this view of duxite genesis was refuted by Havlena (1964) and later by Zelenka (1972): the formation of fossil resins was described as being the sum of pressure and temperature, but only a local temperature increase during coalification was responsible for resin fossilisation, as induced by the composition of the original plant resins. Murchison (Murchison

\* Corresponding author.

E-mail address: [havelcova@irms.cas.cz](mailto:havelcova@irms.cas.cz) (M. Havelcová).

and Jones, 1964; Murchison, 1966) studied samples containing resinites, including duxite, using infrared spectroscopy. Showing aliphatic structures and carbonyl absorption with developing aromatic clusters, duxite was described as thermally metamorphosed resinite created during natural pyrolysis. With regard to duxite, Millais and Murchinson (1969) stated that the duxite's infrared spectrum was very similar to that of alginite present in Scottish boghead coals.

Since the 1970s, duxite discoveries have been reported in botanical structures; cavities of fossilised and coalified trees, stumps and roots; or in pelocarbonate concretions (Zelenka, 1972, 1982; Bouška and Dvořák, 1997; Dvořák and Řehoř, 1997; Dvořák, 1999). The fossil resin substances had a red-brown or brown-black color, a waxy and resinous luster, conchoidal fractures, a melting point of 94–246 °C, a carbon content of 61–84%, and a hydrogen content of 8–17%. Fossil resin discoveries in the area of the Vršany mine, located in another region of the North-Bohemian coal Basin, were published in 1998 with a summary of the physical-chemical properties of samples (Bartoš et al., 1998). These samples differed from the previously discovered duxites in color and carbon content. The authors also mentioned the unusual location of this discovery: inside a charred tree trunk.

Bouška and Dořák then summarised the acquired knowledge and localities of duxite discoveries (Bouška and Dvořák, 1997; Dvořák and Řehoř, 1997; Bouška et al., 1999; Dvořák, 1999) and described new locations in the Medard-Libík coal mine of the Sokolov Basin, confirming reports about findings of such materials in the past in this area (Kuhlwein, 1951). This duxite was located in the cracks of sideritized coalified trees, and the roots and trunks of trees that had traces of fire with coalified and fusinized bark on their surfaces. Physical properties and chemical analyses of the samples confirmed their similarities to those samples from the North Bohemian Basin. The authors concluded that according to variations in melting points, the samples were mixtures of several solid hydrocarbons as a result of diagenetic processes that had occurred in the original resins.

Vávra summarized previous work (Vávra et al., 1997; Vávra, 2009) and added the results of the analyses of new samples from two sites: the Bílina and the Vršany open cast mines. These duxite samples were concentrated in preserved parts of coalified roots and trunks. These samples are highly soluble in organic solvents and are therefore suitable for analysis by GC/MS. Six hydrocarbon compounds were identified as products of the diagenesis of plant terpenes: drimane, C<sub>16</sub>-bicyclic sesquiterpane, labdane, simonellite, retene, and C<sub>18</sub>-tricyclic diterpane. As the compositions of the samples varied extensively, Vávra (2009) concluded that duxite was a mixture of resins and waxes. This author, along with Paclt (1953), therefore included duxite among resinous bitumens. Krumbiegel (2002) also classified duxite as a mixture of bitumen, resins and waxes. Nevertheless, due to its high resin content, duxite can be characterized as an accessory fossil resin, and the basic conditions for duxite formation are the presence of resin in the original plant material and its specific transformation. Information about duxite was most recently summarized by Juríková (2011).

Duxite is not just of local interest because a similar type of Tertiary fossil resin has been documented in Devon (England) and the Lone Valley (California) (Grantham and Douglas, 1980). However, no other detailed investigations of these substances have been carried out. Generally, fossil resin is distinctive for its extraordinary preservation, and the uniqueness of duxite lies in the fact that it is most likely the only fossil resin that can be found directly in trees, i.e. *in situ*. From previously published information about duxite, it is obvious that there are differences in its descriptions and many questions are still unanswered. These include, Can all fossil resins found in the area of the North Bohemian and Sokolov basins be called duxite? Are there any differences between duxites, and if

so, what are they and why? Can duxite have a specified botanical origin? Is it possible to further characterise duxite and speculate on how it was created? Can this information help to evaluate sedimentary or diagenetic conditions?

To answer these questions, a set of duxite samples was collected, including samples from museums. These were analysed by several methods. Because thermal maturation can modify the chemical structure of resins heating experiments were performed to determine the influence of temperature on sample structure and to explain differences in chemical structures among duxites.

## 2. Materials and methods

### 2.1. Samples

Twenty samples of fossil resins, collected from the northwest part of the Czech Republic in the North Bohemian and Sokolov basins, were processed. The set included four samples from museum collections (marked H) from the Emeran mine (samples H01 and H02 - probably originally defined by Doelter in 1874) and other historic samples from a museum in Ústí nad Labem (H03-H04). Fifteen fossil resins (marked D) were of modern findings (since 1988) from the Vršany, Bílina and Nástup Tušimice mines (Most Basin) (D01-D15), and one sample (marked S) from the Medard-Libík mine (Sokolov Basin) (S01). Samples D13, D14, and D15 were the deepest deposits and were collected from the Bílina Mine. All samples were divided into two groups: resins found and collected from trees whose trunks were standing in an upright position, i.e. *in situ*; and resins from trunks stored in sandstones or secondarily deposited material that was transported by water to the site of discovery. The list of the samples with their known descriptions and year of collection is shown in Table 1.

A highly pure duxite sample D08 available in abundance was used for experiments involving carbonisation in air and in inert atmosphere of nitrogen at various temperatures (100–400 °C) for 48 h, to observe changes in sample composition and to help explain chemical differences among samples.

### 2.2. Geological setting

The majority of historical samples described and presented in this paper are Miocene. Their origin is the sedimentary fill of two sub-basins of the Ohře Rift (or Eger Graben) structure – the Most Basin and the Sokolov Basin (Fig. 1). The Most Basin is the largest and deepest of sedimentary basins within the Ohře Rift system. Its volcanic and sedimentary fill was formed from the Oligocene to middle Miocene. The oldest filling (Oligocene) is called the Střezov Formation and is mainly of volcanic origin. The Miocene filling of the basin is called the Most Formation and is divided (Matys Grygar et al., 2014) into the Duchcov Member unit (generally under the main coal seam), the Holešice Member (coal seam and equivalent deltaic to alluvial sediments), the Libkovic Member (monotonous lacustrine clays with illite – smectite above coal seam), the Lom Member (lacustrine clays to coal) and the Osek Member (monotonous lacustrine clays). All newly described samples were found within sediments of the Holešice Member, in clastic sediments in the vicinity of the main coal seam. Samples from the Vršany Mine originate from alluvial conditions of the Žatec Delta system and are slightly older than samples from the lacustrine Bílina Delta – the main coal seam overburden at the Bílina Mine (Mach et al., 2014). The position of the Libík Mine sample from the Sokolov Basin can be defined as Oligocene in age. Usually, duxites from the Vršany and Bílina mines were found within wood permineralised by carbonates (dolomite or siderite) and quartz, often in the form of droplets or other formations indicating flow

**Table 1**  
Description of fossil resins. References are given for samples that have been studied in the past.

Sample	Location	Description	Year of sampling	Reference
<i>North Bohemian basin</i>				
H01	Emeran Mine	Sample from a museum in Ústí nad Labem	1874	Doelter (1874)
H02	Emeran Mine	The originally described duxite ?	1874	Doelter (1874)
H03	Františka Mine	Sample from a museum in Ústí nad Labem	?	
H04	Johan Mine	Sample from a museum in Ústí nad Labem	?	
D01	Bílina Mine	Haulage section, silicified tree	1994	
D02	Bílina Mine	Tree, lying in sands	1991	
D03	Bílina Mine	Tree, lying in sands	1988	
D04	Bílina Mine	Tree from green clays	1989	
D05	Bílina Mine	Tree, standing <i>in situ</i>	1994	
D06	Bílina Mine	Xylitic silicified tree, standing <i>in situ</i>	1994	
D07	Bílina Mine	Silicified tree, drops of quartz cavity	1998	
D08	Vršany Mine	1 cm thick layers in pelocarbonate concretions	1998	
D09	Vršany Mine	Dolomitized tree	1998	
D10	Vršany Mine	Silicified tree	2012	
D11	Vršany Mine	?	?	
D12	Nástup Tušimice	Xylite and duxite on rifts, non-coal lower position	2013	
D13	Bílina Mine	Stump horizon, septarian concretions	2016	
D14	Bílina Mine	Stump horizon, septarian concretions	2016	
D15	Bílina Mine	Stump horizon, septarian concretions	2016	
<i>Sokolov basin</i>				
S01	Medard-Libík	Sideritised and coalified tree	1999	Bouška et al. (1999)

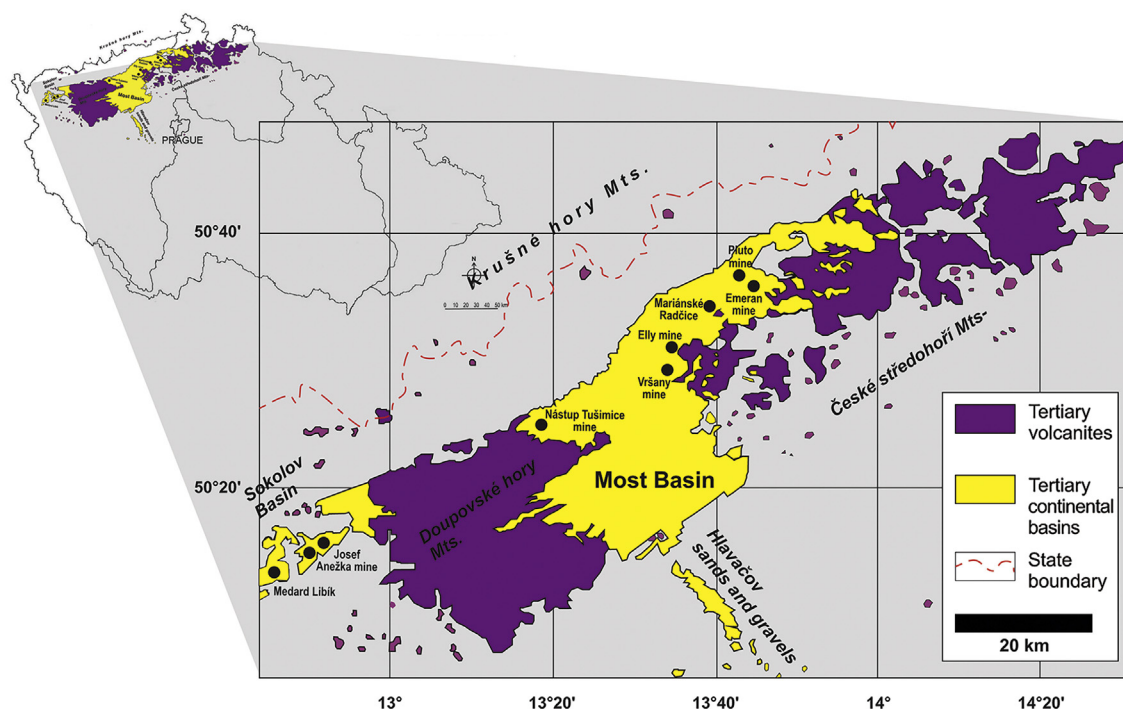


**Fig. 1.** Location of the Miocene continental basins: Most Basin and Sokolov Basin, and position of the mines where the samples were collected.

through radial, tangential or transversal cracks or other cavities. Macroscopic duxite formations were obviously younger than formations of diagenetic minerals.

### 2.3. Methods

Petrographic characterisation consists of a macroscopic description of duxite grains focused on colour and gloss, and micropetrographic analysis, including maceral composition and light reflectance of ulminite and resinite. Small polished sections were prepared from samples that had been studied using an Olympus BX51 optical microscope and an Axio Carl Zeiss microscope with reflected light and photometric and fluorescent arrangements.

The standard procedure (ISO 7404) was used to measure light reflectance of resinite bodies and residues of plant tissues involved in the maceral group of huminite. In the case of coal admixtures, a complete maceral analysis with mineral ingredients was processed (Taylor et al., 1998; Sýkorová et al., 2005; Pickel et al., 2017). Special attention was paid to morphological and optical changes probably caused by weathering.

Elemental compositions of samples were determined on an as-received basis using a CHNS/O micro-analyzer (Thermo Finnigan Flash FA 1112, Italy). The softening point was determined using the Vicat method (Laget, Czech Republic).

Samples (cca 1 g) were dissolved in dichloromethane (Analytika s.r.o., Czech Republic), and 5 $\alpha$ -androstane was added as an internal

quantification standard. The extracts were analysed by GC/MS using a Trace Ultra - DSQ II (ThermoScientific, USA) instrument equipped with a capillary column DB 5 (30 m × 0.25 mm × 0.25 μm film). The GC oven was heated from 35 °C (3 min) to 100 °C at a rate of 8 °C/min and then to 300 °C (5 min) at a rate of 4 °C/min. Helium was used as a carrier gas. Chromatograms and mass spectra were evaluated using the Xcalibur software (ThermoElectron, UK). Identification of compounds was based on comparisons with spectra from the National Institute of Standards and Technology mass spectral library. Biomarkers were quantified in the total ion current (TIC) chromatogram by relating the peak area of the target compound to the peak area of an internal standard of known concentration.

Analytical flash pyrolysis was performed at 610 °C for 20 s, using a CDS Pyroprobe 5150 (CDS Analytical, LLC, USA) pyrolysis unit connected to the GC/MS instrument described above. Both the interface and the transfer lines were heated to 300 °C. The analyses were carried out with a temperature program from 40 °C (3 min) to 210 °C (5 min) at a heating rate of 8 °C/min and then to 300 °C (2 min) at a rate of 20 °C/min. The area of each individual peak was divided by the total area of the integrated TIC and expressed as the relative abundance of the total area, in percent. Selected ion monitoring was also used as a mode of data acquisition. Pyrolysis was combined with methylation (TMAH-Py-GC/MS) using a 25% (w/w) solution of tetramethyl ammonium hydroxide (TMAH) (Sigma-Aldrich).

Fourier transform infrared (FTIR) spectra of the fossil resins samples were collected on a Nicolet 6700 FTIR (Thermo Nicolet Instruments Co.) with a N<sub>2</sub> purging system. Spectra were acquired using a single reflection ATR (Attenuated Total Reflection) GladiATR accessory equipped with a single-bounce diamond crystal (angle of incidence 45°). A total of 64 scans were averaged for each sample and the resolution was 4 cm<sup>-1</sup>. Ratios of the spectra were computed against a single-beam spectrum of the clean ATR crystal and converted into absorbance units using ATR correction. Data were collected within the range 4000–400 cm<sup>-1</sup>. The position and intensity of absorption features in the infrared spectra were identified according to the following references (Beck et al., 1964; Streibl et al., 1976; Socrates, 1994; Ibarra et al., 1996; Brody et al., 2001; Jehlička et al., 2004; Guiliano et al., 2007) and used for designation of the botanical source of resins (Tappert

et al., 2013) and for determination of their degree of fossilisation (Murchison and Jones, 1964; Murae et al., 1996; Murchison, 1966; Lyons et al., 2009).

FT-Raman spectra were obtained using a Nicolet 6700 instrument with the NXR 9650 FT-Raman module attached and Nd<sup>3+</sup>/YVO<sub>4</sub> near infrared excitation at 1064 nm. Spectra were recorded at 4 cm<sup>-1</sup> resolution from 1024 accumulated scans. A nominal laser power of about 0.1 W was used with a spot size of 50 μm.

### 3. Results

#### 3.1. Basic characterization

All samples had elemental compositions (Table 2) that correspond to the maceral group resinite (van Krevelen, 1993; Pickel et al., 2017). Museum samples H01 and H02 (Emeran mine), which can be assumed to be the originally described duxite, had slightly lower contents of carbon and hydrogen together with a higher content of oxygen than the other samples, which differed slightly from the published values (Table S1 in Supplementary Material). The differences in compositions can be explained by previous laboratory methods and by possible natural as well as artificial impurities and weathering of the almost 150-year-old material.

Supplementary data associated with this article can be found, in the online version, at <https://doi.org/10.1016/j.orggeochem.2018.07.014>.

All samples had very good and, for fossil resins, unusual solubilities in dichloromethane (DCM), which in most cases, were almost complete. Softening points of the resins were low and were within the interval from 63 to 143 °C (Table 2).

#### 3.2. Museum samples (H01-H04)

Duxite samples were brittle, had a black color, conchoidal fractures or lumps and a pitch-to-silky shine (Fig. S2 in Supplementary Material). A microscopic study revealed a diversity of the samples, as shown by the presence of residual impurities of coalified tissues or coal matter impacted by sample deposition. Their structures ranged from amorphous masses to fine-grained material blended with other macerals (Table 3; Fig. S3 in Supplementary Material).

**Table 2**

Physico-chemical characterization (carbon, hydrogen, nitrogen and sulfur content, solubility in dichloromethane, and softening points) of the fossil resins: museum samples (H01-H04), fossil resins collected in the North Bohemian Basin from 1988 to 2013 (D01-D15), a sample collected in the Sokolov Basin (S01). \*samples are too small to determine.

Sample	%C	%H	%N	%S	(H/C) <sub>at</sub>	(O/C) <sub>at</sub>	Solubility in DCM (%)	Softening point (°C)
<i>North Bohemian basin</i>								
H01	68.53	7.00	0.55	0.29	1.23	0.26	97	82
H02	76.56	8.65	1.42	0.00	1.36	0.13	99	143
H03	76.92	8.85	1.28	8.01	1.38	0.05	100	81
H04	81.71	10.20	0.43	0.09	1.50	0.07	100	91
D01	83.80	10.66	1.25	0.67	1.53	0.03	99	67
D02	84.21	11.31	1.13	0.74	1.61	0.02	98	54
D03	83.38	10.97	1.87	0.46	1.58	0.03	100	102
D04	81.85	10.43	0.93	0.24	1.53	0.06	100	91
D05	83.54	10.96	0.83	0.00	1.57	0.04	100	63
D06	74.48	9.67	1.65	1.70	1.56	0.13	81	77
D07	83.36	10.89	0.66	0.00	1.57	0.05	100	79
D08	84.38	10.85	0.95	0.31	1.54	0.03	100	65
D09	77.31	9.33	0.82	0.28	1.45	0.12	62	65
D10	84.13	10.69	1.56	1.09	1.52	0.02	79	65
D11	86.17	10.96	0.34	0.04	1.53	0.02	100	63
D12	84.17	9.70	2.30	0.00	1.38	0.03	96	117
D13	87.65	8.65	0.63	0.57	1.18	0.02	69	*
D14	87.53	8.86	0.85	0.25	1.21	0.02	60	*
D15	87.19	8.90	0.74	0.29	1.22	0.02	63	*
<i>Sokolov basin</i>								
S01	85.90	10.14	0.16	0.03	1.42	0.03	100	112

**Table 3**  
Results of petrographic analysis of the fossil resins.  $R_{\text{res}}$  - reflectance of resinite.

Sample	$R_{\text{res}}$	Liptinite (%)	Resinite	Liptodetrinite	Exsudatinit	Bituminite	Suberinite	Sporinite	Huminit (%)	Ulminit	Textinit	Corpohuminit	Attrinit	Inertinit (%)	Funginit	Minerals (%)
North Bohemian basin																
H01	0.14	86.3	56.8	24.0		2.2	2.3	1.0	10.0	1.1	6.7		2.2	1.1	1.1	2.6
H02	0.14	65.4	48.1	13.5		3.8			34.6	17.3	1.9	5.8	9.6			
H03	0.12	100.0	100.0													
H04	0.12	100.0	100.0													
D01	0.13	100.0	100.0													
D02	0.14	85.9	85.9						12.5	10.9	1.6	1.1				1.6
D03	0.15	79.9	79.9						20.1	1.4	17.6					
D04	0.11	100.0	100.0													
D05	0.11	100.0	100.0													
D06	0.13	73.8	73.8						26.2	9.5	16.7					
D07	0.11	100.0	100.0													
D08	0.13	100.0	100.0													
D09	0.12	41.5	39.5	1.5	0.5				8.3	2.0	4.5	0.8	1.8	0.7	0.7	49.5
D10	0.11	69.1	67.0	2.1					18.1	14.5	3.6		1.5			12.8
D11	0.15	100.0	100.0													
D12	0.11	87.7	85.9	1.5				0.3	6.3	2.9	1.3	0.8	1.3			6.0
D13	0.18	100.0	100.0													
D14	0.20	100.0	100.0													
D15	0.19	100.0	100.0													
Sokolov basin																
S01	0.12	52.3	52.3						20.4	12.5	5.7	2.2				27.3

Sample H01 was a resin composed of a diverse mixture of resinite grains of different sizes, up to liptodetrinite and bituminite (lower than 10  $\mu\text{m}$ ), which were connective matter for other macerals – textinite, ulminite ( $R_r = 0.23\%$ ), fragments of cell walls (attrinit), suberinite, sporinite, funginit and quartz grains. Similarly, sample H02 revealed the bright yellow fluorescence of finely grained resinite, liptodetrinite and bituminite, with some different-sized particles of huminit: those from ulminite ( $R_r = 0.21\%$ ), textinite to attrinit (<10  $\mu\text{m}$ ) and corpohuminit. Samples H03 and H04 appeared as 100% resinite. The colour and consistency of the samples changed significantly and rapidly during their microscopic observation due to the heat from the light source of the microscope. The colour varied from tan to yellow or green.

The compositions of samples H01 and H02 were similar but differed considerably from the extracts of samples H03 and H04 (Fig. 2a; Table S4 in Supplementary Material). Sesquiterpenes  $\alpha$ -cedrene,  $\alpha$ -cedrane and cuparene, compounds that are usually restricted to the species Cupressaceae (Otto et al., 2002), can be described as characteristic duxite compounds and were found in extracts of H01 and H02; diterpenes  $\alpha$ (H)-phylocladane (the most abundant diterpane in the H02 extract), simonellite, retene, and 16,17-bisnordehydroabietane were also identified as diagenetic products (biomarkers) of natural terpenoids.

The results of the TMAH-Py-GC/MS analysis confirmed the similarities of samples H01 and H02. Eudesmene and  $\alpha$ -cedrane were the compounds identified as having the highest concentrations, together with other unidentified  $C_{15}$  terpenes (MW 204 and 206) (Fig. 2b; Table S5 in Supplementary Material). Several cyclic compounds were formed as a result of thermal reactions, and other terpenes were the products of the fragmentation of bond-breaking reactions. The fragments produced are assumed to be representative of the original non-volatile compounds.

The chemical structure of H03 was derived from straight and branched chain aliphatic compounds that are typical of natural waxes with an admixture of natural impurities. Pyrolysis of this material led to the production of a typical alkyl series consisting of alkanes, alkenes, and alkadienes originating from esters, decarboxylation of the fatty acid moiety, and the alkenes from the alcohol moiety as a result of scission. The H04 extract contained only traces of sesqui- and diterpenes but more triterpenes. The pyrolytical fingerprint was similar to H03. ATR-FTIR spectra (Fig. 3) also confirmed the similarities of samples H01 and H02 and their dissimilarities from samples H03 and H04.

In the spectral region 3700–3100  $\text{cm}^{-1}$ , a broad envelope of overlapping bands was observed, generated by the stretching vibration of the hydroxyl groups in alcohols and phenols. The positions of two major bands at approximately 3400 and 3200  $\text{cm}^{-1}$ , determined using the second derivative of the spectra, showed structures with different hydrogen bonds. The band intensities of the hydroxyl groups decreased in the order H01 > H02 > H03 = H04, which was consistent with the GC/MS analysis results of the H01 and H02 extracts, showing the presence of phenolic abietane diterpenes (totarol and ferruginol).

Prominent bands of the stretching vibration of the aliphatic C–H bonds were found in the frequency region of 3000–2800  $\text{cm}^{-1}$ . This part of the spectra was composed of five (H03, H04) and six (H01, H02) bands, as demonstrated via curve-fitting by a mixed Gaussian-Lorentz profile function. The two most intense bands at 2922–2926 and 2953–2958  $\text{cm}^{-1}$  were due to the antisymmetric stretching vibrations of the methylene and methyl groups. Those bands at 2845–2850 and 2866–2870  $\text{cm}^{-1}$  were ascribed to the symmetric stretching vibrations of the  $\text{CH}_2$  and  $\text{CH}_3$  groups (Fig. S6 and Table S7 in Supplementary Material).

Other bands of the aliphatic C–H bonds belonged to the deformation vibrations at  $\sim 1460$  and  $\sim 1440$   $\text{cm}^{-1}$ . The additional bands at  $\sim 1410$ – $1415$   $\text{cm}^{-1}$  were ascribed to the vibration of the

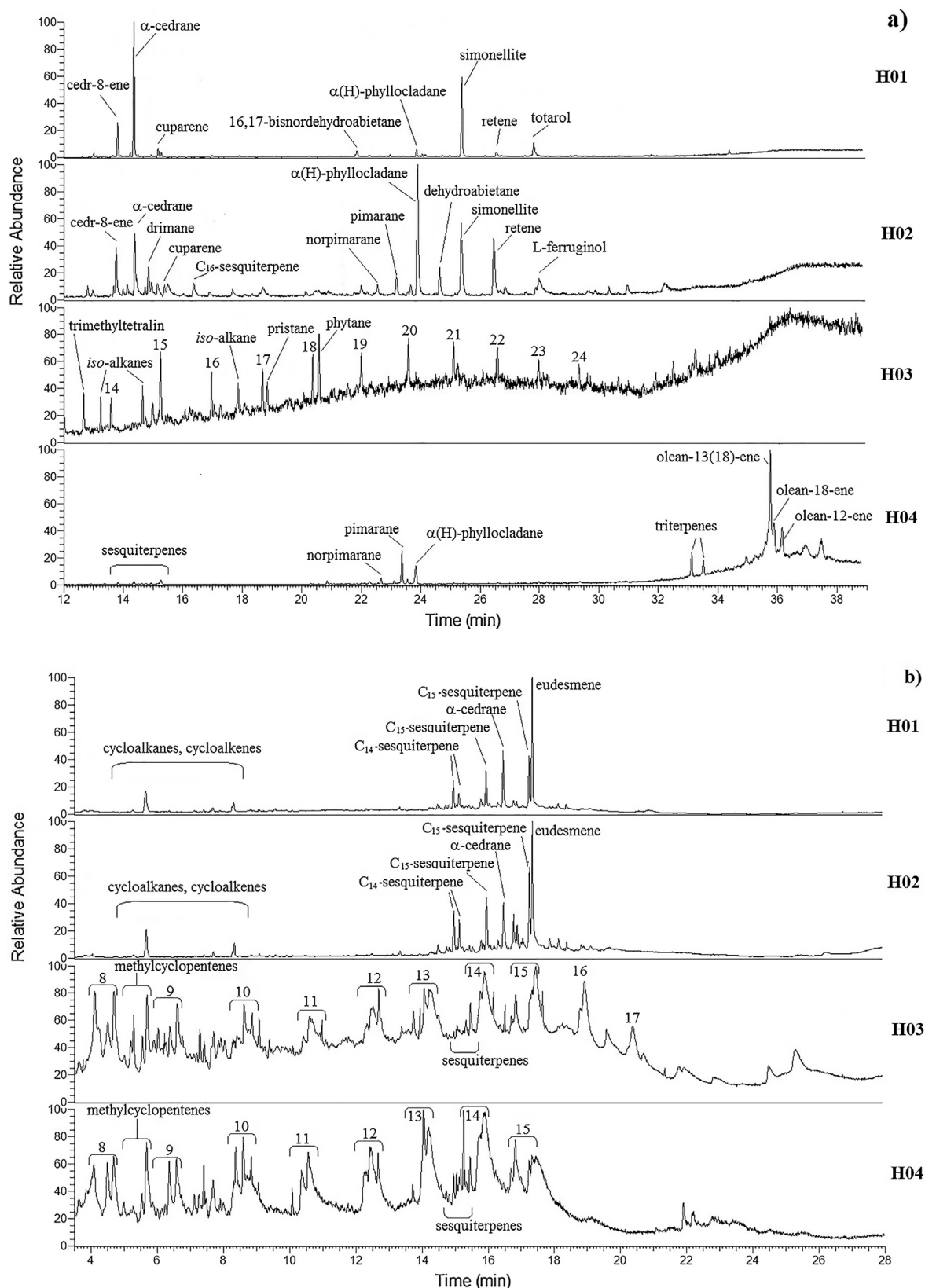


**Fig. 2.** (a) TIC chromatograms of the four museum fossil resin extracts. Peaks identified by carbon number correspond to *n*-alkanes. (b) Pyrograms of the four museum samples. Peaks identified by carbon number correspond to *n*-alkanes, *iso*-alkanes, alkenes, and alkadienes.

methylene group adjacent to the carboxyl group. Bands at  $\sim 1380$  and  $\sim 1360$   $\text{cm}^{-1}$  correspond to geminal methyl groups, e.g., in abietane diterpenes. The frequency region of  $1800\text{--}1500$   $\text{cm}^{-1}$

contained a rich collection of bands that revealed aromatic spectral features. When the aromatic content was high in a given sample, the intensities of the C=O stretching bands of carbonyl compounds

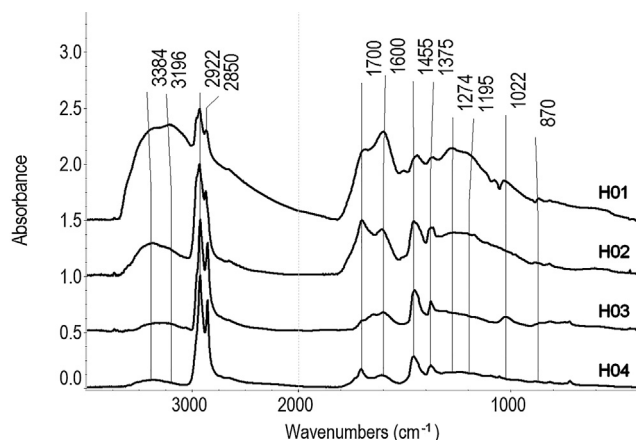


Fig. 3. ATR-FTIR spectra the four museum fossil resins in the region 4000–400  $\text{cm}^{-1}$ .

such as conjugated carbonyls ( $1657\text{--}1668\text{ cm}^{-1}$ ), carboxylic acids ( $1691\text{--}1707\text{ cm}^{-1}$ ), esters ( $1728\text{--}1740\text{ cm}^{-1}$ ) and anhydrides ( $1765\text{--}1767\text{ cm}^{-1}$ ) were relatively weak. The relative aromaticity can be semi-quantitatively described using the intensity of the stretching vibration of aromatic C=C bonds ( $\sim 1600\text{ cm}^{-1}$ ) related to the intensity of bands of aliphatic structures ( $\sim 1460\text{ cm}^{-1}$ ). The aromaticity of the duxite samples decreased in the order  $\text{H01} > \text{H02} > \text{H03} = \text{H04}$ , similar to that of the hydroxyl groups. The results were consistent with high contents of aromatic compounds, as identified by the GC/MS analysis of extracts (retene, simonellite, totatol, ferruginol, dehydroabietane compounds).

In the region of  $1300\text{--}900\text{ cm}^{-1}$ , a large number of overlapping bands were found, belonging predominantly to stretching vibrations of C–O bonds in acids, phenols, alcohols and esters. In addition, these bands were due to the deformation vibrations of the O–H and C–H bonds and the stretching vibration of the ring C–C bonds. The spectral region of  $900\text{--}700\text{ cm}^{-1}$  was also very complex and contained  $\rho(\text{CH}_2)$  rocking bands,  $\delta(\text{CCC})$  deformation vibrations and out-of-plane vibrations of aromatic C–H bonds  $\gamma(\text{C-H})_{\text{ar}}$ . The ATR spectra of the H03 and H04 samples revealed predominant peaks at  $720\text{ cm}^{-1}$  that belonged to the  $\rho(\text{CH}_2)$  rocking vibration in long fatty acid chains.

### 3.3. Contemporary fossil resins collected from 1988 to 2016 (D01–D15, S01)

D01–D15, S01 resins were brittle, reddish or brownish to almost black in color, with pitch-to-silky shines and conchoidal fractures or lumps (Fig. S2 in Supplementary Material). They constituted resinite, amorphous and non-structural masses, in white reflected light or brown colour with reflectance values of 0.11 to 0.20%  $R_{\text{res}}$ , and with yellow to yellow-green fluorescence. A group of samples (D01, D04, D05, D07, D08, D11, D13, D14, D15) consisted of approximately 100 vol% of resinite (Table 3). In the other group of samples (D02, D03, D06, S01), resinite was accompanied by remnants of coalified tissues, likely gymnosperm woods as indicated by the huminite macerals, textinite and ulminite, with reflectances between 0.21% and 0.32%. In the remaining samples, resinite occurred together with huminite macerals with reflectances from 0.20% to 0.26%, rarely with funginite and grains of quartz (D09, D10), and clay minerals (D12) (Fig. S8 in Supplementary Material).

Chromatograms of the sample extracts (except D02 and S01) showed that, the distribution of compounds fit well for all resins (Figs. 4a; S9 and Table S10 in Supplementary Material). The samples differed only in the distribution abundances and quantitative contents of the individual compounds. The important component

in almost all resins was  $\alpha$ -cedrane.  $\text{C}_{20}$  tricyclic terpane (MW 276),  $\text{C}_{18}$  tricyclic diterpane (MW 248), 18-norabieta-7,13-diene (MW 258), labdane (MW 278), 16,17-bisnordehydroabietane (MW 242),  $\alpha(\text{H})$ -phylocladane (274), simonellite (MW 252), and retene (MW 234), which are the products of various stages of diagenesis of natural terpenoids were present in high concentrations. The  $\text{C}_{20}$  tricyclic terpane, a compound with molecular mass 276, was identified on the basis of its mass spectrum by comparison to that shown by Philp (1985), similar to  $\text{C}_{18}$  diterpane with a molecular mass of 248. The S01 sample did not contain compounds distinctively different from those of other extracts, but their distribution was distinct.

The composition of the D02 sample extract was different (Fig. 4a): typical sesqui- and diterpenes were in minor abundance, and a series of unknown compounds was observed and were tentatively identified as a terpenoid series according to their mass spectrometric fragmentation patterns and molecular weights of 406, 408, and 410, all with a very strong main peak at 191.

The results of TMAH-Py-GC/MS were very consistent for all samples (Figs. 4b; S11 and Table S12 in Supplementary Material). Contrary to the analysis of the extracts, the fingerprints of samples D02 and S01 coincided with those of other samples. Many terpenes could not be identified.  $\text{C}_{15}$  sesquiterpene (MW 206), eudesmene (MW 204), and  $\alpha$ -cedrane (MW 206) were identified as the compounds with the highest concentrations of pyrolysis products.

All contemporary samples showed similar spectral features and differed only in the relative band intensities of their aromatic structures and oxygen functional groups (OH, COOH). The spectra had more resolved bands than the museum duxite samples, as seen in the representative ATR-FTIR spectrum for sample D08 (Fig. 5), and these could be ascribed to greater freshness of the samples with varying degrees of aromatization and oxidation. The features of the stretching vibrations of the aliphatic C–H bonds were very similar to the spectra of the museum samples H01 and H02, differing only in the higher intensities in this area. The deformation vibrations of the aliphatic CH bonds had a characteristic pattern, forming eight bands at  $1471, 1458, 1441, 1416, 1387, 1376, 1363$  and  $1344\text{ cm}^{-1}$ , which were the average values obtained by curve-fitting of all thirteen samples (Table S7 in Supplementary Material).

Sharp bands were found in the frequency region of  $900\text{--}700\text{ cm}^{-1}$ , belonging to the deformation vibrations of the  $\text{CH}_2$  and  $\text{CH}_3$  groups and/or out-of-plane vibrations of the aromatic C–H bonds. According to GC/MS analysis, the extract of sample D08 contained a large amount of retene (54%) and therefore bands at  $885, 829, 796, 754,$  and  $716\text{ cm}^{-1}$ , corresponding mainly to this compound. The bands in this region were ascribed to the out-of-plane vibration of isolated (1H,  $885\text{ cm}^{-1}$ ), two adjacent (2H,  $829\text{ cm}^{-1}$ ) and three neighboring (3H,  $798\text{ cm}^{-1}$ ) aromatic hydrogen atoms. The intensity of the band at  $885\text{ cm}^{-1}$  might also be increased by the contribution of exomethylene  $\omega(\text{C}=\text{CH}_2)$  vibrations in labdane structures, as labdane was identified by GC/MS. Spectral features between  $900$  and  $700\text{ cm}^{-1}$  also differed within individual samples, and these differences could be attributed to differences in the content of simonellite ( $1 \times 1\text{H}, 1 \times 2\text{H}$ ), dehydroabietane diterpenes ( $1 \times 1\text{H}, 2 \times 2\text{H}$ ) and totarole ( $1 \times 2\text{H}$ ).

### 3.4. FT-Raman spectra

The high fluorescence partly or completely obscured Raman signals, which is typical for biological samples. Despite this difficulty, useful spectra from duxites S01 and D02 were obtained (Fig. 6; Table S7 in Supplementary Material). A highly aromatic character was observed by Raman spectroscopy. The important bands appear centered at approximately  $1450\text{ cm}^{-1}$  and  $1645\text{ cm}^{-1}$  and are assigned to the C=C stretching of double bonds and aliphatic

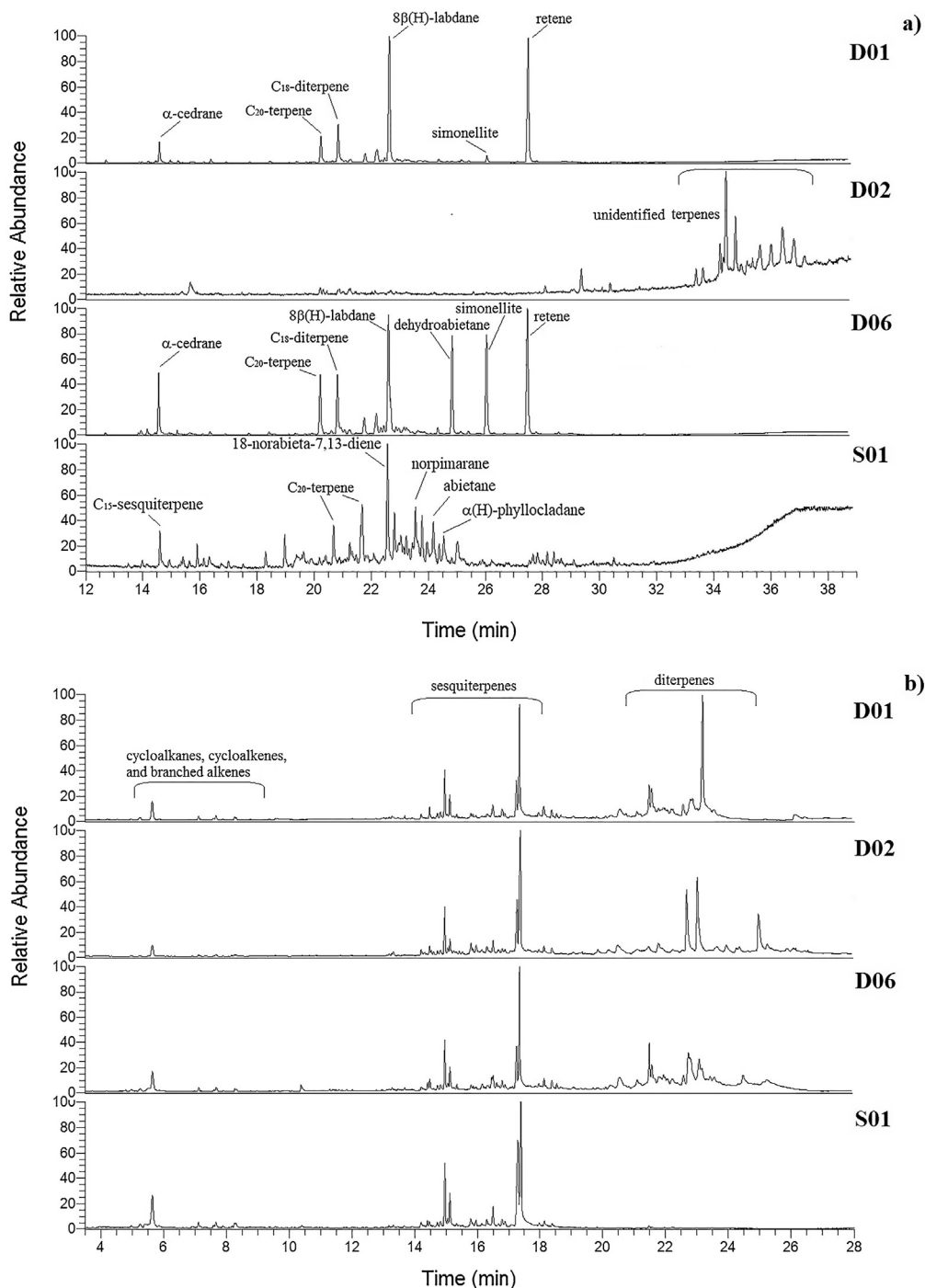


Fig. 4. (a) Example of TIC chromatograms for fossil resin extracts D01, D02, D06, S01. (b) Example of pyrograms for samples D01, D02, D06, S01.

C—H bending, respectively. Their ratio could be useful for guessing the maturation of the samples.

### 3.5. Altered fossil resin

To evaluate the hypothesis that resin compositions have been influenced by various conditions during their burial histories, including temperature, sample D08 was heated under atmospheres of nitrogen and air. The loss of resin mass increased with temperature, and thermal stress had an expected impact on the elemental composition: the hydrogen content decreased with increasing temperature, the carbon content decreased in air and increased in nitrogen, and the oxygen content distinctly increased in air. This

progression is seen in the van Krevelen diagram using the  $(H/C)_{at}$  and  $(O/C)_{at}$  ratios (Fig. 7). The predominant result of the thermal treatment was a reduction in sample solubility.

Only sesquiterpene reduction accompanied by small changes in diterpene intensities appeared in the extract analysis after heating at temperatures from 150 to 300 °C in nitrogen (Fig. 8). The more labile structures were destroyed and evaporated as volatiles. The main changes in chromatographic spectra occurred at 400 °C: the only two compounds identified in this extract were longifolene and 16,17-bisnordehydroabietane. This sample, heated at 400 °C/nitrogen, showed a significant increase in the degree of aromatisation without significant changes in the infrared spectral band intensities of the oxygen functional groups at ~1770, ~1740

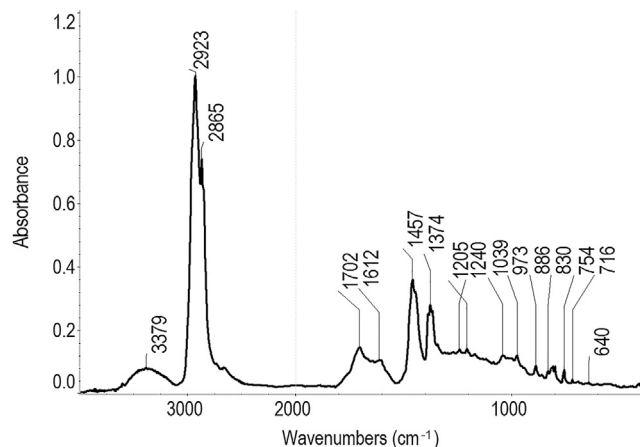


Fig. 5. ATR-FTIR spectrum of the duxite sample D08 in the region 4000–400  $\text{cm}^{-1}$ .

and  $\sim 1700 \text{ cm}^{-1}$  (anhydrides, esters and acids) (Fig. 9); the bands of highly conjugated compounds ( $1668 \text{ cm}^{-1}$ ) and double bonds ( $1640 \text{ cm}^{-1}$ ) disappeared completely while the aliphatic C–H content was reduced by approximately half. These results were consistent with a rapid decrease in  $(\text{H}/\text{C})_{\text{at}}$  ratios corresponding to the dehydroaromatisation of the aliphatic C–H structures. The infrared spectrum also showed distinct bands of out-of-plane aromatic C–H in the  $900\text{--}700 \text{ cm}^{-1}$  region (not shown). Resinite reflectance also increased continuously (Table 4).

At  $200\text{--}250 \text{ }^\circ\text{C}$  in air, the sample extract revealed a  $\alpha$ -cedrane reduction that was counterbalanced by the appearance of cedrene oxide. The degree of aromatisation increased, and the content of oxygenated functional groups doubled, as shown by ATR-FTIR analysis. The aromatic diterpenes simonellite and retene declined, and 18,19-bisnorsimonellite appeared, as did 16,17-bisnordehydroabietane. Samples heated to  $400 \text{ }^\circ\text{C}$  revealed no compounds in their extracts. Aliphatic C–H bonds ( $I_{\text{C-H}} = 3\%$ ) were lost almost completely at  $300 \text{ }^\circ\text{C}$ . Resinite reflectance increased continuously, as did the reflectance of oxidized rims (Table 4). Changes in sample composition by heating were also demonstrated by TMAH-Py-GC/MS (Supplementary Material S13 and S14).

## 4. Discussion

### 4.1. Can we label all fossil resins found in the area of the North Bohemian and Sokolov basins as duxite?

According to the results of all the analyses except those for museum samples H03 and H04, we can conclude that all the fossil

resins studied showed consistent compositions, including the sample originally defined in 1874 as duxite. Samples H03 and H04 from the Františka and Johan mines had completely different chemical compositions (Fig. 2a). The chemical structure of H03 showed mainly straight and branched cyclic compounds that are typical for natural waxes. The chemical compositions of most natural waxes are complex and comprise a wide variety of long-chain alkanes, esters, polyesters and hydroxy esters of long-chain primary alcohols and fatty acids. The low softening point (as was also confirmed by softening in the light source of the microscope) is typical for them (Table 2). The extract of H04 contained only traces of sesqui- and diterpenes but more triterpenes were found as an admixture of natural impurities (Fig. 2a). The pyrolytic fingerprint of H04 is similar to that of H03 (Fig. 2b): the analyses of these materials led to the production of a typical alkyl series consisting of alkanes, alkenes from the alcohol moiety as a result of scission, and alkenes originating from esters and the decarboxylation of the fatty acid moiety.

### 4.2. Why have differences been found in the duxite results?

Samples displayed various anomalies. The fusion, migration, and redeposition of the original resin ejections led to the occurrence of duxite in cracks and crevices in the form of coatings, lumps and drops within fossil trees. These duxite substances, preserved as orange and brown matter, were close to authentic resin. However, the originally described duxite samples (now museum samples) were almost black, or a dark color, as mentioned in Doelter (1874) and Jurasky (1940). These were excavated from coal mines as a resin insertion or in veins intersecting coalbeds. The low transparency and black coloration with a system of fine cracks of these samples can be attributed to alterations during secondary burial in the coal seam (Pastorelli et al., 2012).

When Vávra et al. (1997) performed the first GC/MS duxite analysis, they reported that the samples studied were far from homogenous and that their compositions probably varied; this was confirmed in the present study. The presence of  $\alpha(\text{H})$ -phyllocladane (Figs. 2a, and S2 in Supplementary Material) is an example of an advanced stage in the metamorphic history of the resins. This compound was the most abundant compound in the H02 total extract and was present in the H01, D13, D14, D15, and S01 extracts but was not detected in the other duxite extracts. Labdanoic acids and other labdane derivatives and isomers, common components in all conifers (Otto and Wilde, 2001), can be assumed to be precursors of  $\alpha(\text{H})$ -phyllocladane. As labdane was identified in several duxite samples (Table S10 in Supplementary Material), the occurrence of  $\alpha(\text{H})$ -phyllocladane can be explained by the degradation and aging of the labdane structures. The pres-

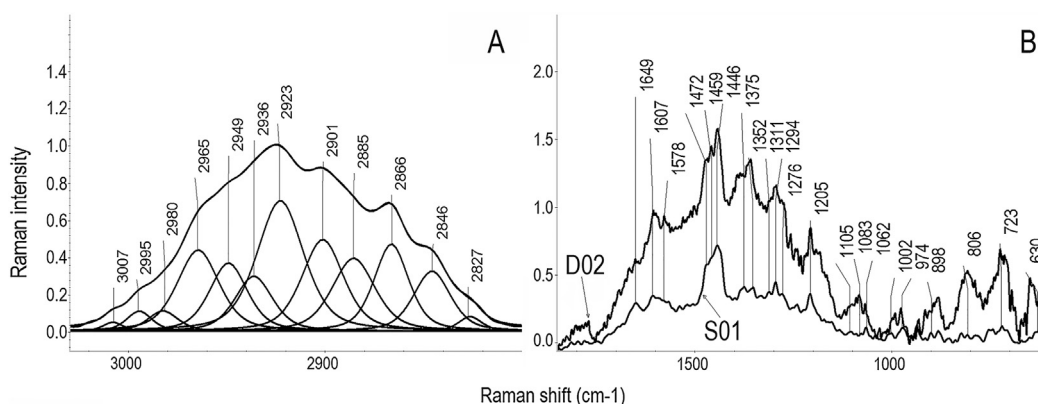
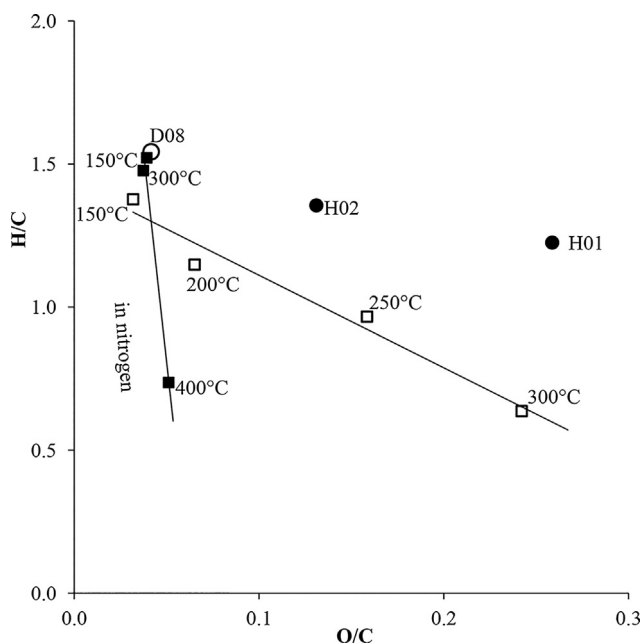


Fig. 6. Curve-fitted FT-Raman spectrum of duxite S01 in the region  $3050\text{--}2800 \text{ cm}^{-1}$  (A), and spectra of D02 and S01 samples in the region  $1850\text{--}600 \text{ cm}^{-1}$  (B).



**Fig. 7.** van Krevelen diagram showing changes in atomic H/C and O/C ratios after heating of sample D08 in air and in nitrogen. For comparison, samples H01 and H02 were added. ○ sample D08; □ sample D08 after heating in air; ■ sample D08 after heating in nitrogen; ● H01 and H02.

ence of  $\alpha$ (H)-phyllocladane corresponded to the state and position of the samples, as it was identified in samples from the deepest part of the Břilina Mine (D13, D14, D15) or found in a coalified tree from the Medard-Libík mine (Sokolov Basin) (S01).

Variations in band intensities of aromatic and aliphatic structures found in the FTIR spectra for contemporary duxite samples were only several percent, but they emerged more in the case of hydroxyl groups, carboxylic acids and conjugated carbonyls (approximately 5%). Atomic ratios of  $(H/C)_{at}$ , related to the level of aromatic structures in the samples (Fig. 10A), demonstrated higher aromaticities in the H01 and H02 museum samples. The higher contents of OH and COOH functional groups were also related to the  $(O/C)_{at}$  ratio, showing the highest values for the H01 and H02 samples (Fig. 10B). This may be due to the presence of ferruginol and totarol in these samples. Although these phenolic diterpenes are naturally produced (Cox et al., 2007), in this case, they seem to be the result of air access during their post-burial history, including post-excavation history, as oxidative changes can lead to their formation (Langenheim, 2003).

To show resistance or proclivity to sample modification, sample D08 was heat treated: the distribution of biomarkers did not change until 300 °C/nitrogen or 250 °C/air; only the intensities of some compounds differed (Fig. 8). 16,17-bisnordehydroabietane appeared in the GC spectrum after 400 °C/nitrogen treatment, probably as a diagenetic product from abietane-type precursors (abietane, abietic acid, ferruginol) and is an indicator of the oxidative alteration of the resin (Otto et al., 2002). These results suggest that this feature may be used as an indicator of general alteration, regardless of the environment. Longifolene is a naturally occurring hydrocarbon found primarily in pine resins and is thermally resistant among sesquiterpenes (Francis et al., 2012). It seems that this compound was a product of rearrangement during the thermal alteration of D08.

The relative abundances of aliphatic C–H, aromatic C=C bonds and carbonyl C=O groups for the thermally altered and nonaltered duxite samples were described using peak intensities at  $\sim 1450$ ,  $\sim 1600$  and  $\sim 1700$   $\text{cm}^{-1}$ , which were related to the sum of their

intensities ( $\Sigma I_{1450} + I_{1600} + I_{1700} = 1$ ). The results summarised the impacts of temperature on the presence of functional groups in the samples (Fig. 11). According to this functional composition, the museum sample H02 is located on the heat-oxidation shift in the diagram, close to sample D08, which was heated to 250 °C under an air-containing atmosphere. The museum sample H01 was structurally shifted more towards the D08 sample pyrolyzed under a nitrogen atmosphere, resulting in higher aromaticity and relatively low aliphatic C–H linkage.

#### 4.3. Can the botanical origin of duxite be specified?

It is known that gymnosperms have evolved constitutive and inducible mechanisms to produce resins that help in both wound healing and defense against attack by bark beetles and other organisms (Hudgins et al., 2003). Large varieties of terpenoids and/or phenolic compounds are components of resins that vary both across and within species due to individual terpene synthases (Keeling and Bohlmann, 2006a, 2006b). Some of these compounds, under suitable conditions, resist the processes of fossilisation and coalification. The diversity in the compositions of the original resins arises from their ability to fossilize. Usually, fossilisation begins by combining monomers across terminal groups to form a polymeric complex, resulting in naturally polymerized fossil resin (Langenheim, 2003). However, small amounts of fossil resins are the result of the preservation of non-polymerizable terpenoids. Duxite seems to be a part of this group, as was mainly confirmed by the high solubility of the matter. Duxite is 17.5–20 million years old and is found within Miocene sediments (Matys Grygar et al., 2014). Fossilised tree trunks from sites with duxite findings were classified as belonging to the Cupressaceae (s.l.) family, i.e., *Glyptostrobus europaeus*, *Quasisequoia couttsiae*, and *Taxodium dubium* (Teodoridis and Sakala, 2008; Havelcová et al., 2013). Duxite was often found close to the foliage and/or cone scales of *Taxodium dubium* (Kvaček et al., 2004), and the relevance to this type of tree species appears clear.

The most abundant constituents of the natural resins of the Cupressaceae family are largely members of three structural groups of the abietanes, pimaranes, and dehydroabietanes (Otto and Wilde, 2001), all of which are characterised by tricyclic parental skeletons with endocyclic double bonds (in Supplementary Material Fig. S15). Members of all three diterpene types were identified in the duxite extracts and, together with the sesquiterpenes  $\alpha$ -cedrene, cuparene and  $\alpha$ -cedrane (in Supplementary Material Table S10), confirmed that the duxite samples are fossilised exudates from a member of the Cupressaceae conifer family. The distinction of the chemical compositions among other amber forms is visible in their comparisons using Py-GC/MS (Anderson and Winans, 1991; Anderson et al., 1992).

The spectroscopic differences among plant resins from conifer families reflect differences in the underlying skeletal structures of their terpenoid compounds. For example, the presence of a prominent and sharp band at  $\sim 2850$   $\text{cm}^{-1}$  of CH<sub>2</sub> groups in the infrared spectra points to Cupressaceae tree resin (Tappert et al., 2011, 2013). Other bands of aliphatic C–H bonds revealed in the spectral region 1500–1300  $\text{cm}^{-1}$  could be used to determine the botanical origins of resins: the band of the deformation vibration of the CH<sub>2</sub>/CH<sub>3</sub> at  $\sim 1450$   $\text{cm}^{-1}$ , being greater than the band intensity of the methyl groups at  $\sim 1370$   $\text{cm}^{-1}$ , is typical for resin of the Cupressaceae family. Spectra of Pinaceae tree resins show the opposite trend. Using data from Tappert et al. (2011) and the results of the samples studied here, the contemporary duxite samples showed results that were clearly close to those ratios for the Cupressaceae family (Fig. 12). The remote position of the waxy museum samples H03 and H04 confirms that these samples are visibly differentiated by their chemical composition.

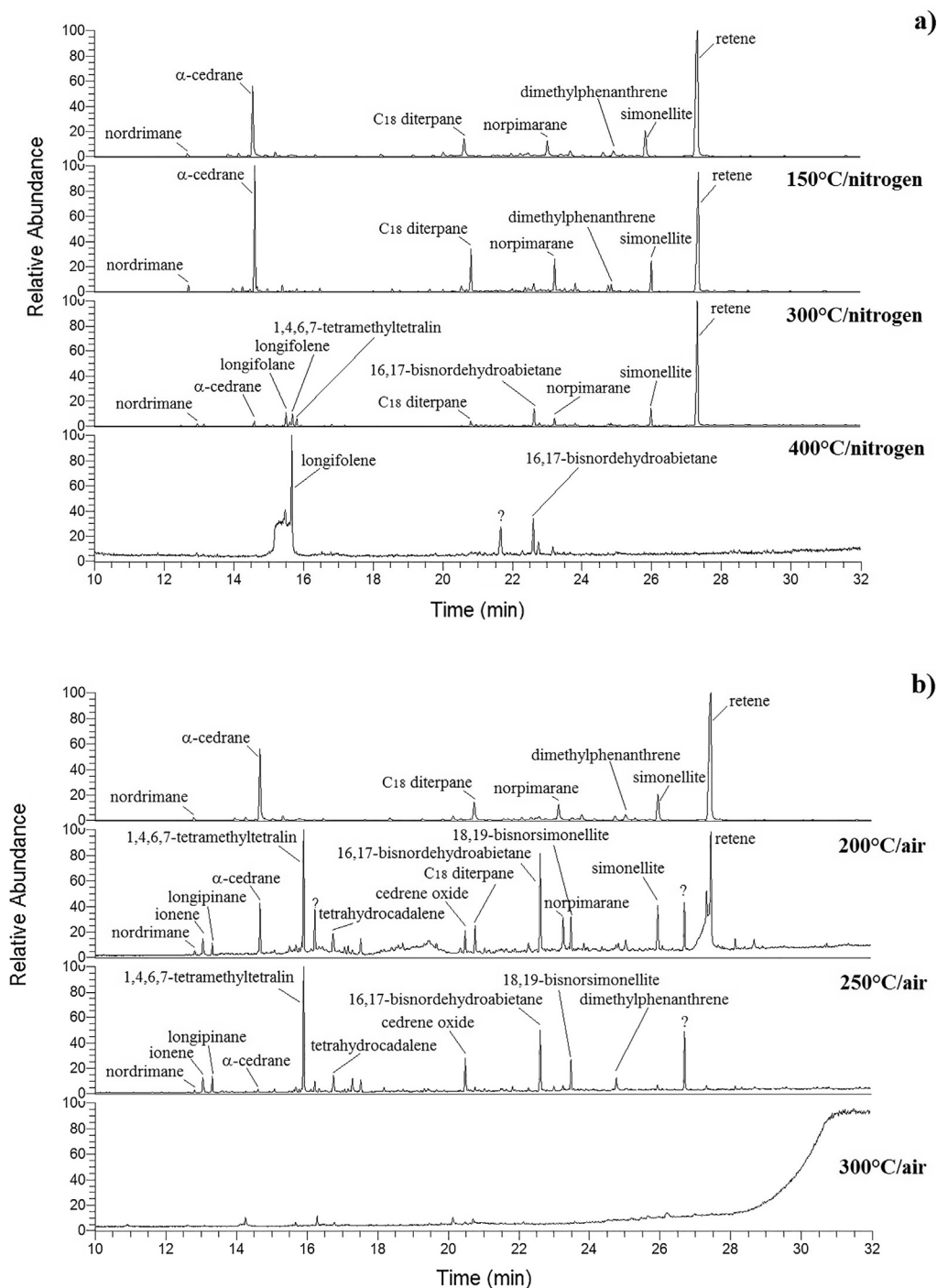
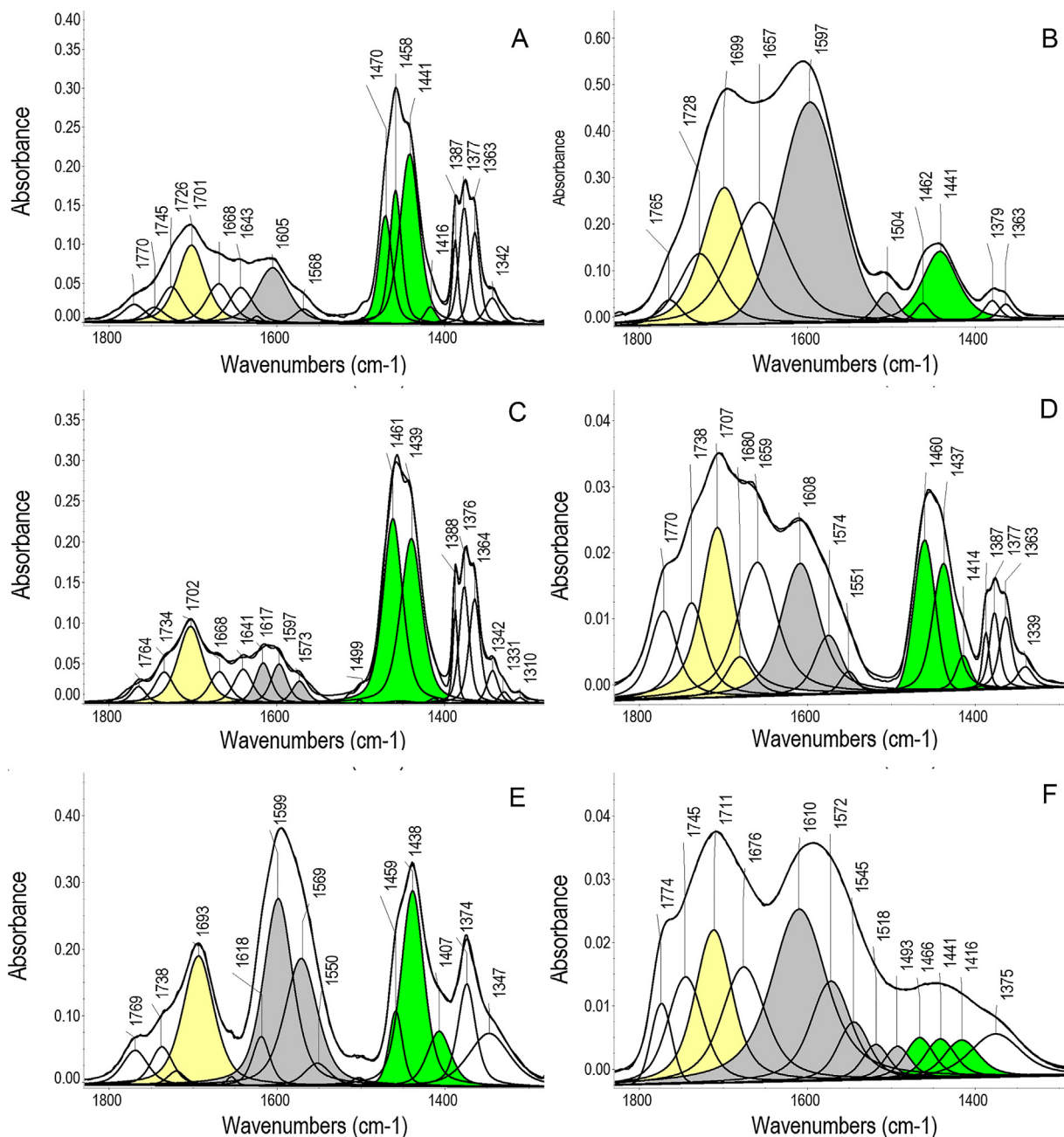


Fig. 8. Total ion chromatograms of D08 extracts showing the distribution of compounds after heating in nitrogen (a) and in air (b).

#### 4.4. Is it possible to further characterize duxite?

A very interesting characteristic of duxite is its very high solubility (Table 2). The dissolution of polymers depends on their physical properties and chemical structures (molecular weight, polarity, branching, and degree of crosslinking) (Miller-Chou and Koenig, 2003). As the degree of crosslinking or molecular weight increases, the solubility of a polymer in a solvent decreases at a particular temperature. From this point of view, duxite is not a polymerised material or is at a very early stage of polymerisation. This was supported by the FTIR analysis because the most often used spectroscopic evidence of polymerisation - linking related diterpene

units into polymer chains - is the presence of an exocyclic methylene group with an absorption band at  $\sim 890\text{ cm}^{-1}$ ; the intensity of this band in the FTIR spectra was very low (Table S7 in Supplementary Material), confirming the presence of only low levels of polymerization in the samples. According to Langenheim (2003), resins with high abietane or pimarane contents are believed to be subject to oxidative degradation or dehydrogenation and not to be involved in the formation of the ambers polymeric structure. However, the presence of conjugated double bonds in the structures of abietanes does not exclude these compounds from forming a molecular complex that consists of a few monomer units, such as diabetic acid (Llevot et al., 2015).



**Fig. 9.** Curve-fitted ATR-FTIR spectra of the duxite samples in the region of 1800–1300  $\text{cm}^{-1}$ : sample D08 (A), sample H01 (B), sample D08 heated at 300 °C/nitrogen (C), sample D08 heated at 250 °C/air (D), sample D08 heated at 400 °C/nitrogen (E), sample D08 heated at 300 °C/air (F).

The highly aromatic character of duxite could be observed from the Raman spectra (Fig. 6). The ratio calculated from the band intensities at 1645  $\text{cm}^{-1}$  (C=C stretching of double bonds) and 1450  $\text{cm}^{-1}$  (aliphatic C–H bending) was suggested to indicate the maturity and degree of oxidation of the fossil resins (Brody et al., 2001; Winkler et al., 2001; Jehlička et al., 2004) because this ratio decreases due to the loss of double bonds with increasing maturation. The values of the ratio  $I_{1645}/I_{1450}$  varied in the case of the duxite samples, falling between 0.30 (D02) and 0.45 (S01), which are relatively low values and approach that of the Cenomanian fossil resin muckite, with its ratio of 0.48 (Jehlička et al., 2004).

Anderson and co-workers (Anderson and Winans, 1991; Anderson et al., 1992) created a classification system for fossil

resins. Most fossil resins from around the world have been grouped into classes with polymeric skeletons. However, there are also fossil resins that fall into Class IV and V of the classification that do not have a polymeric structure. Retinites from European brown coals are included in Class V, with abietane and primarane skeletons forming the fossil resin (Beck, 1999). Cenomanian Moravian amber, Oligocene amber from Devon (England), and Pliocene amber from the Lone Valley (California) are members of Class IV (Streibl et al., 1976; Grantham and Douglas, 1980). The solubilities of these fossil resins were 20–46% in pyridine and 50–80% in DCM, and the published results showed the presence of  $\alpha$ -cedrene, cedrane, cuparene, cedren-10-one, 8 $\beta$ H-cedran-9-one and cuparenic acid in resin extracts. These analyses (Grantham and Douglas, 1980) are in close agreement with the results presented in this work.

**Table 4**  
Reflectance values and composition of products of thermal alteration in air and in nitrogen.

	Loss of matter (%)	Solubility (%)	Reflectance of altered resinite $R_{res}$ (%)	Reflectance of oxidation rims $R$ (%)	Non-altered resinite (vol.%)	Altered resinite with changed fluorescence (vol.%)	Altered resinite without fluorescence (vol.%)
D08		100.0	0.13	0.00	100.0	0.0	0.0
D08 in 150 °C/air	25	88.5	0.18	0.24	98.2	1.8	0.0
D08 in 200 °C/air	25	0.5	0.22	0.28	8.3	90.2	1.5
D08 in 250 °C/air	42	0.4	0.24	0.42	0.0	75.0	25.0
D08 in 300 °C/air	75	0.1	0.28	0.68	0.0	33.8	66.2
D08 in 150 °C/nitrogen	20	5.1	0.16	0.00	99.4	0.6	0.0
D08 in 300 °C/nitrogen	27	4.8	0.19	0.00	0.0	64.4	35.6
D08 in 400 °C/nitrogen	84	0.1	0.74	0.00	0.0	0.0	100.0

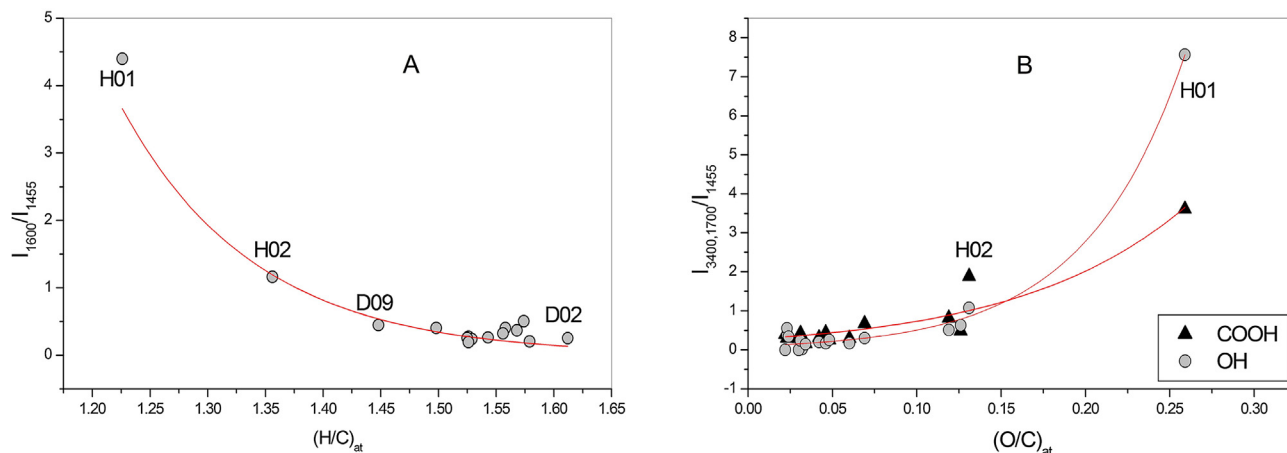


**Fig. 10.** Correlation of ATR-FTIR structural duxite parameters and atomic ratios: (A) aromaticity ( $I_{1600}/I_{1455}$ ) vs.  $(H/C)_{at}$ , and (B) OH content ( $I_{3400}/I_{1455}$ ) and COOH content ( $I_{1700}/I_{1455}$ ) vs.  $(O/C)_{at}$ .

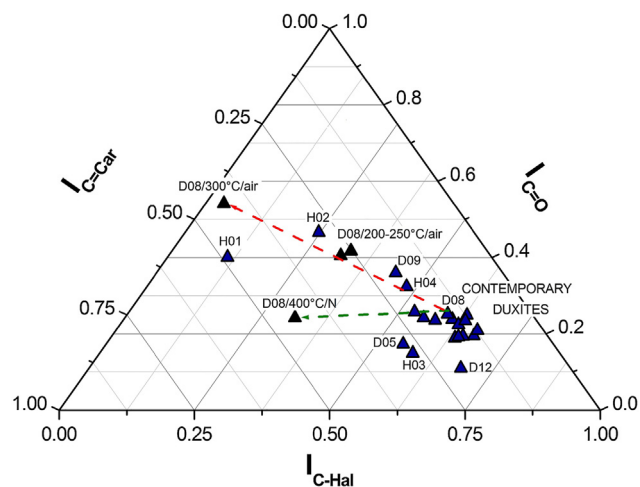


**Fig. 11.** Ternary diagram demonstrating changes in the relative abundance of aliphatic C–H bonds, carbonyl groups, and aromatic C=C bonds. The green arrow indicates the direction of changes in chemical composition for samples prepared under atmosphere of nitrogen; the red arrow indicates the direction of changes under atmosphere of air. (For interpretation of the references to colour in this figure legend, the reader is referred to the web version of this article.)

#### 4.5. How was duxite formed?

Resin ducts are common in gymnosperms that produce resin as a local terpenoid response induced by mechanical wounding, abiotic stress, attack by insects or pathogens, or fungal inoculation. Specific terpenoids may also be induced and emitted systemically

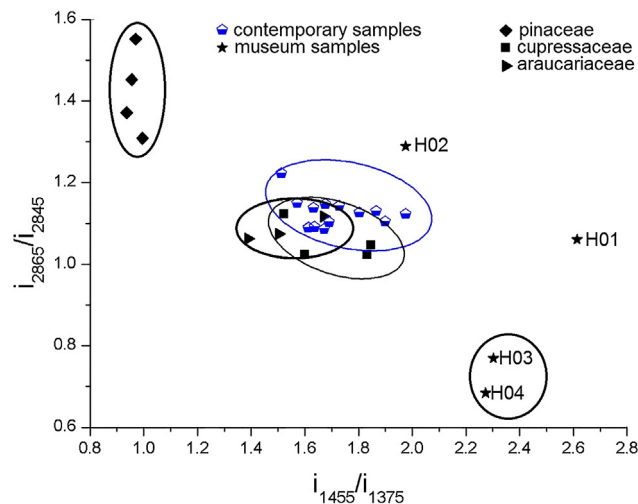


**Fig. 12.** Band ratios plot using intensities of valence and deformation vibrations in FTIR spectra showing differences for museum and contemporary duxite samples. Data for modern resins were added for comparison using results according to Tappert et al. (2011).

as volatiles (Keeling and Bohlmann, 2006a, 2006b; Rodríguez-García et al., 2014). When exposed to light and air, resins have hardened because the most volatile components have evaporated, while the non-volatile compounds are preserved. Usually, oxidation-degradation reactions and polymerization influence the resin structure. However, duxite is not polymerised, as most other

ambers are. It seems that the respective compounds could only create dimers or smaller oligomers, and thus, duxite remained largely soluble. Light intensity and UV radiation can cause further changes via cleavage reactions, cross-linking and or aromatisation (Langenheim, 2003; Scalarone et al., 2003) that affects the chemical structure, similar to the rapid warming of duxite (without light) in this study. The solubility of duxite samples significantly decreased after simulated heating, reflectance increased even after slight warming, and alterations in fossil resin were reflected by changes in fluorescence.

Gymnosperms were common land vegetation during the Miocene. Trees and resin preserved *in situ* or transported and deposited in quiet water sediments formed at the bottom of rivers, fluvial lakes or lagoons. Wet sediments of clay and sand preserved trees and resin well because access to oxygen was limited. Therefore, if suitable resin producing trees and appropriate burial conditions were combined, the resin was preserved and is associated with layers of fossil wood and woody sub-bituminous coal. The climatic optimum was documented in the Middle Miocene when a warm temperate and humid climate increased resin exudation (Hradecký and Brázdil, 2016), as is known from recent forests in warm subtropical or tropical climates.

Fossilised resins from around the world were mostly located in secondary deposits, and from this point of view, the findings of duxite are unique because contemporary duxite materials have been found inside fossil tree trunks. These fossil woods were mineralised, replacing organic materials with minerals (siderite, quartz or dolomite). This is probably why duxite stayed inside the mineralised trunks, although resin material secondarily migrated during burial. Because no minerals were found in the duxite samples, migration had to occur after mineralogical processes or at the very end of the crystallization of minerals. In addition, septarian cracks, where duxite was located in some cases, occurred at late stages of the concretion formations.

#### 4.6. Can these results help to evaluate sedimentary or diagenetic conditions?

From a geological point of view, information about temperatures achieved during diagenesis and basin development is important but often unknown. However, it is difficult to draw conclusions about diagenetic pathways of resinous organic matter and assess the effects of sedimentary environments on diagenesis because of the complexity of biogeochemical processes in the geosphere. Geothermal stress is one of the important factors influencing structural changes in resins and their accumulation within the Earth's crust. The thermal effects of vulcanism on the environment can be ruled out in the Most Basin, which started to function as a sedimentary basin at the Oligocene/Miocene boundary. At that time, the main phase of volcanic activity in the adjacent volcanic centers had almost ceased (Suhr, 2003). Only thermal spring activity is documented in the area of the Most Basin (Mach et al., 2017), and some mineral springs could reach temperatures of approximately 45–70 °C, as is known from syngenetic limestones. The softening points of the resins studied were higher (approximately 63–143 °C), representing the minimum temperatures for resin movement within the sediment layers and mineralised trees. The maximum temperature could be estimated to not exceed 250 °C in an air-containing atmosphere. However, due to the overall chromatographic record showing the presence of oxides and some unidentified compounds, the sedimentary environment seemed to have been more air-limited, so the temperature could have reached 300 °C. This would have had an impact on the resinous organic matter and led to small variations among samples. This temperature seems to be high, but the temperature conditions combined with the pressure had a significant and unexpected

effect on resin deposition. During the time when resins migrated, they could have contained more volatile compounds that would have had an impact on resin viscosity. At the same time, increasing pressure could have helped prevent the escape of volatile compounds.

## 5. Conclusions

The fossil resinduxite had previously only been studied using basic physico-chemical methods and GC/MS analysis of sample extracts. Duxite is material found mainly within trees and the uniqueness of this material demands more detailed research. GC/MS was complimented by Py-GC/MS, ATR-FTIR spectroscopy, Raman spectroscopy and petrographical observations in this study. The set of samples included samples from museum collections and those of modern findings from two localities.

With two exceptions, all studied materials revealed similar molecular fingerprints, proving a relationship between them. The two exceptions were museum samples whose history was not known, but it was important to analyse them to determine differences and to check whether all materials were as originally collected.

The apparent variability in distribution and intensities of identified compounds and functional groups were ascribed to their distinct metamorphic histories. A thermal influence on material transformation was evident from laboratory experiments. Although experimentally, high temperatures were used in combination with high pressure, natural processes can be similar. On the assumption that duxite originated from resin of an almost uniform chemical composition, the identified heterogeneities were caused by fossilisation processes in the post-depositional history of the resins.

Duxite is soluble in organic solvents, from which it follows that it is not typically polymeric material. The distinctive compound in duxite is  $\alpha$ -cedrane, identified in duxite chromatograms as well as in all pyrograms. The classification system of fossil resins is based mainly on the Py-GC/MS method, and according to the results, duxite is a member of Class IV resinites. A tree of the Cupressaceae family is the source of the natural resin, containing abietane, pimarane, and dehydroabietane compounds, and these were identified in the duxite extracts.

## Acknowledgements

This work was carried out thanks to the Operational Program Prague—Competitiveness, project “Centre for Texture Analysis” (No.: CZ.2.16/3.1.00/21538), and to the long-term conceptual development of research organisation RVO: 67985891. The study was financially supported by Severočeské doly, a.s. The authors are grateful to John Brooker for reviewing and correcting the manuscript. We thank anonymous reviewers and Editors (Kliti Grice and Erdem Idiz) for constructive reviews and suggestions that helped to improve the manuscript.

Associate Editor—Kliti Grice

## References

- Anderson, K.B., Winans, R.E., 1991. Nature and fate of natural resins in the geosphere. I. Evaluation of pyrolysis-gas chromatography mass spectrometry for the analysis of natural resins and resinites. *Analytical Chemistry* 63, 2901–2908.
- Anderson, K.B., Winans, R.E., Botto, R.E., 1992. The nature and fate of natural resins in the geosphere—II. Identification, classification and nomenclature of resinites. *Organic Geochemistry* 18, 829–841.
- Bartoš, P., Šulcek, P., Rehoř, M., 1998. Findings of fossil resin of duxite at the Vrřany mine. *Zpravidaj Hnědé uhlí*, 48–53 (in Czech).

- Beck, C.W., 1999. The chemistry of amber. *Estudios Del Museo De Ciencias Naturales De Alava* 14, 33–48.
- Beck, C.W., Wilbur, E., Meret, S., 1964. Infra-red spectra and the origin of amber. *Nature* 201, 256–257.
- Bittner, H., 1913. Streifzüge im Reich der Steine und Versteinerungen. *Lotos: Zeitschrift für Naturwissenschaften* 61, 79–83 (in German).
- Bouška, V., Dvořák, Z., 1997. Minerals of North Bohemian Basin, Prague pp. 88–94 (in Czech).
- Bouška, V., Galek, R., Rojčík, P., Sýkorová, I., Vašíček M., 1999. The find of duxite in the Sokolov Basin. *Bulletin Mineralogicko-Petrologického Oddělení Národního Muzea* 7, 139–142 (in Czech).
- Brody, R.H., Edwards, H.G.M., Pollard, A.M., 2001. A study of amber and copal samples using FT-Raman spectroscopy. *Spectrochimica Acta A* 57, 1325–1338.
- Cox, R.E., Yamamoto, S., Otto, A., Simoneit, B.R.T., 2007. Oxygenated di- and tricyclic diterpenoids of southern hemisphere conifers. *Biochemical Systematics and Ecology* 35, 342–362.
- Doelter, C., 1874. Harz aus der Braunkohle von Dux. *Verhandlungen der Kaiserlich-Königlichen Geologischen Reichsanstalt* 24, 145–146 (in German).
- Dvořák, Z., 1999. Duxite - Czech fossil amber. *Mineral* 7, 366–367 (in Czech).
- Dvořák, Z., Řehoř, M., 1997. Mineralization of fossilized trees of North-West Bohemia. *Zpravodaj Hnědé uhlí*, 47–55 (in Czech).
- Francis, G.W., Christy, A.A., Øygarden, J., 2012. Pyrolytic formation of polycyclic aromatic hydrocarbons from sesquiterpenes. *Food Chemistry* 135, 1316–1322.
- Graham, P.J., Douglas, A.G., 1980. The nature and origin of sesquiterpenoids in some tertiary fossil resins. *Geochimica Cosmochimica Acta* 44, 1801–1810.
- Guliano, M., Asia, L., Onorati, G., Mille, G., 2007. Applications of diamond crystal ATR FTIR spectroscopy to the characterization of ambers. *Spectrochimica Acta A* 67, 1407–1411.
- Havelcová, M., Sýkorová, I., Bechtel, A., Mach, K., Trejtnarová, H., Žaloudková, M., Matysová, P., Blažek, J., Boudová, J., Sakala, J., 2013. Stump Horizon- in the Bílina Mine (Most Basin, Czech Republic) – GC-MS, optical and electron microscopy in identification of wood biological origin. *International Journal of Coal Geology* 107, 62–77.
- Havlena, V., 1964. *Geology of Coal Deposits*. Prague. (in Czech)
- Hradecký, J., Brázdil, R., 2016. Climate in the past and present in the Czech lands in the Central European Context. In: Pánek, T., Hradecký, J. (Eds.), *Landscapes and Landforms of the Czech Republic*. Springer International Publishing, Switzerland, pp. 19–20.
- Hudgins, J.W., Christiansen, E., Franceschi, V.R., 2003. Induction of anatomically based defense responses in stems of diverse conifers by methyl jasmonate: a phylogenetic perspective. *Tree Physiology* 24, 251–264.
- Ibarra, J.V., Munoz, E., Moliner, R., 1996. FTIR study of the evolution of coal structure during the coalification process. *Organic Geochemistry* 24, 725–735.
- Jehlička, J., Jorge Villar, S.E., Edwards, G.H.M., 2004. Fourier transform Raman spectra of Czech and Moravian fossil resins from freshwater sediments. *Journal of Raman Spectroscopy* 35, 761–767.
- Jurasky, K.A., 1940. Der Veredlungszustand der sudetenländischen Braunkohlen als Folge vulkanischer Durchwärmung. *Mitteilungen der Reichsstelle für Bodenforschung* 20, 54–75 (in German).
- Juríková, T., 2011. Duxite - Czech amber. *Gemologický spravodajca* 1, 15–19 (in Slovak).
- Keeling, C.I., Bohlmann, J., 2006a. Diterpene resin acids in conifers. *Phytochemistry* 67, 2415–2423.
- Keeling, C.I., Bohlmann, J., 2006b. Genes, enzymes and chemicals of terpenoid diversity in the constitutive and induced defence of conifers against insects and pathogens. *New Phytologist* 170, 657–675.
- Krumbiegel, G., 2002. Duxite, fossil resin? *Przegląd Geologiczny* 50, 237–239 (in Polish).
- Kuhlwein, F.L., 1951. Influence of volcanic heat on the rank of Bohemian brown coal. *Fuel* 30, 25–30.
- Kvaček, Z., Dvořák, Z., Mach, K., Sakala, J., 2004. Třetihorní rostliny severočeské hnědouhelné pánve. *Granit, Praha*, pp.158 (in Czech).
- Langenheim, J.H., 2003. *Plant Resins: Chemistry, Evolution, Ecology, and Ethnobotany*. Timber Press Inc, pp. 141–194.
- Lievot, A., Grau, E., Carloti, S., Grelier, S., Cramail, H., 2015. Dimerization of abietic acid for the design of renewable polymers by ADMET. *European Polymer Journal* 67, 409–417.
- Lyons, P.C., Mastalerz, M., Orem, W.H., 2009. Organic geochemistry of resins from modern Agathis australis and Eocene resins from New Zealand: diagenetic and taxonomic implications. *International Journal of Coal Geology* 80, 51–62.
- Mach, K., Žák, K., Teodoridis, V., Kvaček, Z., 2017. Consequences of Lower Miocene CO<sub>2</sub> degassing on geological and paleoenvironmental settings of the Ahníkov/Merkur Mine paleontological locality (Most Basin, Czech Republic). *Neues Jahrbuch für Geologie und Paläontologie - Abhandlungen* 285 (3), 235–266.
- Mach, K., Teodoridis, V., Matys Grygar, T., Kvaček, Z., Suhr, P., Standke, G., 2014. An evaluation of palaeogeography and palaeoecology in the Most Basin (Czech Republic) and Saxony (Germany) from the late Oligocene to the early Miocene. *Neues Jahrbuch für Geologie und Paläontologie - Abhandlungen* 272 (1), 13–45.
- Matys Grygar, T., Mach, K., Schnabl, P., Pruner, P., Laurin, J., Martinez, M., 2014. A lacustrine record of the early stage of the Miocene Climatic Optimum in Central Europe from the Most Basin, Ohře (Eger) Graben, Czech Republic. *Geological Magazine* 151, 1013–1033.
- Millais, R., Murchison, D.G., 1969. Properties of the coal macerals: infra-red spectra of alginates. *Fuel* 48, 247–258.
- Miller-Chou, B.A., Koenig, J.L., 2003. A review of polymer dissolution. *Progress in Polymer Science* 28, 1223–1270.
- Murae, T., Shimokawa, S., Aihara, A., 1996. Pyrolytic and spectroscopic studies of the diagenetic alteration of resinates. In: Anderson, K. (Ed.), *Amber, Resinite, and Fossil Resins*. ACS Symposium Series. American Chemical Society, Washington, DC.
- Murchison, D.G., 1966. Properties of coal macerals: infrared spectra of resinates and their carbonized and oxidized products. In: Gould, R.F. (Ed.), *Coal Science*. American Chemical Society, *Advances in Chemistry Series* 55, pp. 307–331.
- Murchison, D.G., Jones, J.M., 1964. Resinite in bituminous coals. *Advances in Organic Geochemistry* 55, 49–69.
- Otto, A., Simoneit, B.R.T., Wilde, V., Kunzmann, L., Püttmann, W., 2002. Terpenoid composition of three fossil resins from Cretaceous and Tertiary conifers. *Review of Palaeobotany and Palynology* 120, 203–215.
- Otto, A., Wilde, V., 2001. Sesqui-, di-, and triterpenoids as chemosystematic markers in extant conifers – a review. *The Botanical Review* 67, 141–238.
- Paclt, J., 1953. A system of caustolites. *Tschermaks mineralogische und petrographische Mitteilungen* 3, 332–347.
- Pastorelli, G., Richter, J., Shashoua, Y., 2012. Evidence concerning oxidation as a surface reaction in Baltic amber. *Spectrochimica Acta A* 89, 268–269.
- Philp, R.P., 1985. *Fossil Fuel Biomarkers*. Elsevier, New York.
- Pickel, W., Kus, J., Flores, D., Kalaitzidis, S., Christanis, K., Cardott, B.J., Misz-Kennan, M., Rodrigues, S., Hentschel, A., Hamor-Vido, M., Crosdale, P., Wagner, N., 2017. Classification of liptinite – ICCP System 1994. *International Journal of Coal Geology* 169, 40–61.
- Rodríguez-García, A., López, R., Martín, J.A., Pinillos, F., Gil, L., 2014. Resin yield in Pinus pinaster is related to tree dendrometry, stand density and tapping-induced systemic changes in xylem anatomy. *Forest Ecology and Management* 313, 47–54.
- Scalarone, D., Lazzari, M., Chiantore, O., 2003. Ageing behaviour and analytical pyrolysis characterisation of diterpene resins used as art materials: Manila copal and sandarac. *Journal of Analytical and Applied Pyrolysis* 68–69, 115–136.
- Socrates, G., 1994. *Infrared Characteristic Frequencies*. J. Wiley & Sons, Chichester.
- Stach, E., 1966. Der Resinit und seine biochemische Inkohlung. *Fortschritte in der Geologie von Rheiland und Westfalen*, Krefeld, pp. 921–968 (in German).
- Streibl, M., Vašíčková, S., Herout, V., Bouška, V., 1976. Chemical composition of cenomanian fossil resins from Moravia. *Collection of Czechoslovak Chemical Communications* 41, 3138–3145.
- Suhr, P., 2003. The Bohemian Massif as a Catchment Area for the NW European Tertiary Basin. *Geolines* 15, 147–159.
- Sýkorová, I., Pickel, W., Christanis, K., Wolf, M., Taylor, G.H., Flores, D., 2005. Classification of huminite–ICCP system 1994. *International Journal of Coal Geology* 62, 85–106.
- Tappert, R., McKellar, R.C., Wolfe, A.P., Tappert, M.C., Ortega-Blanco, J., Muehlenbachs, K., 2013. Stable carbon isotopes of C3 plant resins and ambers record changes in atmospheric oxygen since the Triassic. *Geochimica Cosmochimica Acta* 121, 240–262.
- Tappert, R., Wolfe, A.P., McKellar, R.C., Tappert, M., Muehlenbachs, K., 2011. Characterizing modern and fossil gymnosperm exudates using micro-Fourier transform infrared spectroscopy. *International Journal of Plant Sciences* 172, 120–138.
- Taylor, G.H., Teichmüller, M., Davis, A., Diesel, C.F.K., Littke, R., Robert, P., 1998. *Organic Petrology*. Gebrüder Borntraeger, Berlin-Stuttgart, pp. 209–226.
- Teodoridis, V., Sakala, J., 2008. Early Miocene conifer macrofossils from the Most Basin (Czech Republic). *Neues Jahrbuch für Geologie und Paläontologie - Abhandlungen* 250, 287–312.
- van Krevelen, D.W., 1993. *Coal*. third ed. Elsevier Science Publishers.
- Vávra, N., 2009. The chemistry of amber – facts, findings and opinions. *Annalen des Naturhistorischen Museums in Wien* 111 A, 445–474.
- Vávra, N., Bouška, V., Dvořák, Z., 1997. Duxite and its geochemical biomarkers (“chemofossils”) from Bílina open-cast mine in the North Bohemian Basin (Miocene, Czech Republic). *Neues Jahrbuch für Geologie und Paläontologie-Monatshefte* 4, 223–243.
- Winkler, W., Kirchner, E.Ch., Asenbaum, A., Musso, M., 2001. A Raman spectroscopic approach to the maturation process of fossil resins. *Journal of Raman Spectroscopy* 32, 59–63.
- Zelenka, O., 1972. Fossil resins in the North Bohemian Basin. *Zprávy a studie Okresního vlastivědného muzea Teplice* 8, 19–28 (in Czech).
- Zelenka, O., 1982. The problem of the origin of duxite in the North Bohemian Brown-coal Basin. *Časopis pro Mineralogii a Geologii* 27, 295–299 (in Czech).